Supplementary Information

Distributed Acoustic Transmission Line Approach

In electromagnetism, a dielectric medium can be modeled using a distributed transmission line (TL) network [1]. The basic unit cell in the transmission line is composed of serial impedances and shunt admittances as shown in Fig.S1. The 2D telegrapher's equation for the distributed structure in a two-dimensional (2D) cylindrical coordinate can be expressed as

$$\frac{\partial V}{r\partial \phi} = -I_\phi Z_\phi \tag{S1a}$$

$$\frac{\partial V}{\partial r} = -I_r Z_r$$

$$\frac{1}{r}\frac{\partial}{\partial r}(rI_r) + \frac{1}{r}\frac{\partial I_\phi}{\partial \phi} = -VY \tag{S1b}$$

Where V is the voltage, I_r, I_ϕ are the currents along r and ϕ direction respectively, Z_r, Z_ϕ are the impedance per-unit length along radial and angular direction and Y is the admittance per-unit length.

Now consider the 2D Maxwell equations for transverse magnetic (TM) polarization in cylindrical coordinates with anisotropic but diagonal permittivity and permeability tensors

$$\frac{\partial E_z}{r\partial \phi} = -j\omega\mu_r H_r \tag{S2a}$$

$$\frac{\partial E_z}{\partial r} = j\omega\mu_\phi H_\phi$$

$$\frac{1}{r}\frac{\partial}{\partial r}(rH_\phi) - \frac{1}{r}\frac{\partial H_r}{\partial \phi} = j\omega\varepsilon_z E_z \tag{S2b}$$

Comparison of the above two sets of equations shows that (S1) and (S2) can be mapped to each other under the variable exchange

$$E_z \leftrightarrow V \quad H_r \leftrightarrow I_\phi \quad H_\phi \leftrightarrow -I_r \quad j\omega\mu_r \leftrightarrow Z_\phi \quad j\omega\mu_\phi \leftrightarrow Z_r \quad j\omega\epsilon_z \leftrightarrow Y \tag{S3}$$

The exact equivalence implies that a solution to the 2D cylindrical Maxwell equations above is also a solution to the 2D telegrapher's equation under the above replacement. This further indicates that we can

implement a transformation-based inhomogeneous and anisotropic medium using a cylindrical TL by modifying the value of distributed impedance and admittance accordingly.

A 2D cylindrical cloak is designed to squeeze the cylindrical region into an annular region where r and are the radial coordinate in the original and transformed system respectively. The coordinate transformation leads to the following cloaking parameters [2] in a TL model

$$\frac{Z_r}{Z_0}=\frac{r}{r-R_1} \qquad \frac{Z_\phi}{Z_0}=\frac{r-R_1}{r} \qquad \frac{Y}{Y_0}=\left(\frac{R_2}{R_2-R_1}\right)^2\frac{r-R_1}{r} \tag{S4}$$

Where are the impedance and admittance of the background medium.

Substitute (S1a) into (S1b),

$$\frac{1}{r}\frac{\partial}{\partial r}\left(\frac{r}{YZ_r}\frac{\partial V}{\partial r}\right)+\frac{1}{r^2}\frac{\partial}{\partial \phi}\left(\frac{1}{YZ_\phi}\frac{\partial V}{\partial \phi}\right)=V \tag{S5}$$

We observed that there are different sets of TL which can hold the same voltage distribution as long as the value of and are kept constant. Therefore, we are allowed to use the simplified parameter in Eq.S6 to facilitate the experimental implementation to approximate the cloaking functionality.

$$\frac{Z_r}{Z_0}=0.5 \qquad \frac{Z_\phi}{Z_0}=0.5\left(\frac{r-R_1}{r}\right)^2 \qquad \frac{Y}{Y_0}=2\left(\frac{R_2}{R_2-R_1}\right)^2 \tag{S6}$$

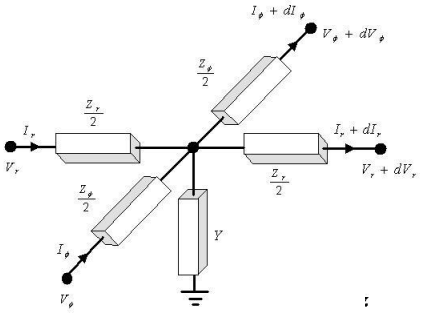

Fig.S1. Unit cell for a 2D distributed transmission line.

Lumped Network Approach

The anisotropic transmission line mentioned in previous section can be physically implemented by a lumped circuit network. Lumped transmission line network have been employed to demonstrate negative index lens to focus electromagnetic [1] and acoustic waves [3].

In order to control ultrasound waves, we propose to build an acoustic TL network by a 2D array of the building blocks as shown in Fig.S2 (a). In each unit cell that is much smaller than the operational wavelength, the cavity with large volume in center works as an acoustic capacitor whereas the channels connecting to four neighboring cells act as serial inductors [4, 5]. An acoustic element can be predominantly of either capacitance or inductance nature, depending on the relative compressibility of the fluid inside the element. Consequently, when an incident acoustic wave is applied onto the fluid in the channels, the pressure gradient through the channels is much greater than that inside the cavity. Hence, it is as if the fluid in the cavity were at rest relative to those in the channels. So when the plug of fluid in the channels oscillates as a unit, there are adiabatic compressions and rarefactions of the fluid inside the larger cavity. Such an acoustic system is analogous to an inductor–capacitor (LC) circuit as shown in Fig.2S (b). The unit cells are positioned periodically along diagonal direction in a cylindrical coordinate to construct a cylindrical cloak. Based on the lumped circuit model, the propagation of the acoustic waves through the unit cell in Fig. S2 (a) can be written as,

$$\frac{\partial P}{\partial r} \approx \frac{P_{n+1,m} - P_{n-1,m}}{\Delta r} = -\frac{j\omega L_r S_r u_r}{\Delta r} \qquad \text{(S7a)}$$

$$\frac{\partial P}{r\partial \phi} \approx \frac{P_{n,m+1} - P_{n,m-1}}{r\Delta \phi} = -\frac{j\omega L_\phi S_\phi u_\phi}{r\Delta \phi}$$

$$\frac{1}{r}\frac{\partial}{\partial r}\left(rS_r u_r\right) + \frac{1}{r}\frac{\partial (S_\phi u_\phi)}{\partial \phi} \approx \frac{r_{n+1}S_{r\,n+1,m}u_{r\,n+1,m} - r_n S_{r\,n-1,m}u_{r\,n-1,m}}{r_n \Delta r_n} + \frac{S_{\phi n,m+1}u_{\phi n,m+1} - S_{\phi n,m-1}u_{\phi n,m-1}}{r_n \Delta \phi_m} = -\frac{j\omega C\, P}{\Delta r}$$

(S7b)

where u_r, u_ϕ are r and ϕ component of velocity , $S_r = t_r w_r$,$S_\phi = t_\phi w_\phi$ are cross section areas, L_r and L_ϕ are acoustic inductance, C is acoustic capacitance and ω is angular frequency.

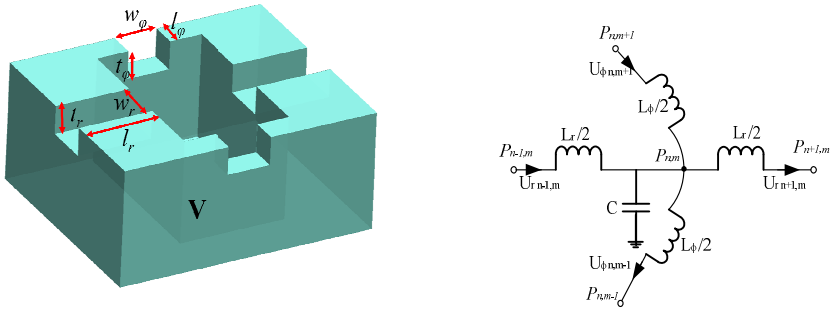

(a) (b)

Fig.S2. (a) One unit cell for an anisotropic acoustic TL network and (b) the corresponding lumped circuit element.

Compared the above equations with the 2D telegrapher's equation Eq. S1, assume which can be easily achieved in the design, we find the lumped circuit elements for this distributed acoustic system interpreted as

$$Z_r = \frac{j\omega L_r S_r}{\Delta r} \quad Z_\phi = \frac{j\omega L_\phi S_\phi}{r\Delta\phi} \quad Y = \frac{j\omega C}{\Delta r S_r} \tag{S8}$$

In this analog, the pressure and particle velocity are mapped to the voltage and current in which the motion of the fluid is equivalent to the behavior of the current in the lumped circuit.

By tailoring the acoustic circuit elements according to Equ.S6, we can physically implement the simplified acoustic cloak by the 2D array of cavities and connecting channels. Substitute Equ.S8 into Equ.S6, we get the condition for the serial inductor and shunt capacitor to construct an acoustic cloak

$$L_r = \rho_w \frac{\Delta r}{2S_r} \quad L_\phi = \rho_w \frac{r\Delta\phi}{2S_\phi}\left(\frac{r-R_1}{r}\right)^2 \quad C = 2\Delta r S_r \beta_w \left(\frac{R_2}{R_2-R_1}\right)^2 \tag{S9}$$

According to the definition of the acoustic inductance and capacitance [6, 7]

$$L_r = \rho_w \frac{l_r}{S_r} \qquad L_\phi = \rho_w \frac{l_\phi}{S_\phi} \qquad C = \frac{V}{\rho_w c_w^2} \tag{S10}$$

Where is the density of water and is sound speed in water, , are channel length along r and ϕ direction and V is the volume of the large cavity. In the lumped circuit model, the aluminum is assumed as

acoustically rigid, which is a good approximation considering the acoustic impedance ρc of aluminum is around eleven times of that of water. A more careful analysis including elasticity of the solid suggested that at low frequency the majority of acoustic energy can be predominantly confined in the fluid, when such an excitation originates from the liquid. [8] On the other hand, aluminum does participate in the wave propagation, and may increases the loss of cloaking material [9].

Substitute (S10) into (S9) yields,

$$\frac{l_r}{\Delta r}=\frac{1}{2} \qquad \frac{l_\phi}{r\Delta\phi}=\frac{1}{2}\left(\frac{r-R_1}{r}\right)^2 \qquad \frac{V}{\Delta r S_\phi}=2\left(\frac{R_2}{R_2-R_1}\right)^2 \tag{S11}$$

Equ.S10 indicates the dependence of inductance and capacitance on the structure geometry and filling medium which is water in the experiment. Therefore, this discrete network allows for a practical implementation of an anisotropic cloak based on lumped circuit model in Equ.S9 by modifying the geometry and placement of the building blocks in the 2D network as shown in Equ.S11.

Effective Material Parameters Based on Transmission Line Network

In an inviscid medium, the two-dimensional (2D) time harmonic acoustic wave equations in a cylindrical coordinate are

$$\frac{\partial P}{r\partial\phi}=-j\omega\rho_\phi u_\phi \tag{S12a}$$

$$\frac{\partial P}{\partial r}=-j\omega\rho_r u_r$$

$$\frac{1}{r}\frac{\partial}{\partial r}(ru_r)+\frac{1}{r}\frac{\partial u_\phi}{\partial\phi}=-j\omega\beta P \tag{S12b}$$

Where P is pressure, $\mathbf{u}$ is particle velocity, β is compressibility, ρ_r ρ_ϕ is density along radial and angular direction respectively.

Compared the above equations with Eq. S7a-S7b, we find the effective density and compressibility of the transmission line can be interpreted as

$$\rho_{eff,r} = \frac{L_r S_r}{\Delta r} \qquad \rho_{eff,\phi} = \frac{L_\phi S_\phi}{r\Delta\phi} \qquad \beta_{eff} = \frac{C}{S_r \Delta r} \tag{S13}$$

Equ.S13 indicates the realization of the metamaterial cloak with the spatially varying parameter profile by tailoring the geometry of the corresponding building blocks. Please note that the effective mass density $\rho_{eff,r}$ is mainly a measure of response through water flow in the narrow channels to the pressure gradients along the radial direction. A similar argument can be applied for the effective density $\rho_{eff,\phi}$ along the angular direction. By modifying the geometry of the narrow channels, the effective mass density along the angular direction for the cloak can be spatially varying. Therefore the anisotropy of mass density is readily introduced in our metamaterial cloak. On the other hand, the effective dynamic compressibility depends on the compliance of the large cavity between the connecting channels. It enables rerouting the paths of underwater sound around the cloaked object without significant scattering by combination of the above effective anisotropic density and compressibility. Such non-resonant scheme is not yet achieved in the optical cloaking experiments.

Sample Fabrication

The 2D acoustic circuit network consisting of an array of large volume cavities and connecting channels is machined in an aluminum plate with the cells positioned periodically along diagonal direction in a cylindrical coordinate. The cloak with radial gradients is approximated by 16-step piecewise homogeneous cylinders. The first ring along the inner boundary of the cloak is composed of 32 cells around the circumference. To keep unit cell size along angular direction smaller than λ/10, starting from the second layer ,the number of unit cells around the circumference is doubled to 64, and increased again to 128 from the sixth layer. The geometry of the sample is listed in table 1. For all the unit cells, the depth and width of the channels $w_r, t_r, w_\varphi, t_\varphi$ are constant value of 0.5mm. The inner radius of the cloak is 13.5mm. We noted that with the same design approach, cloak with larger inner radius is feasible, but with much larger number of unit cells needed to build the cloak.

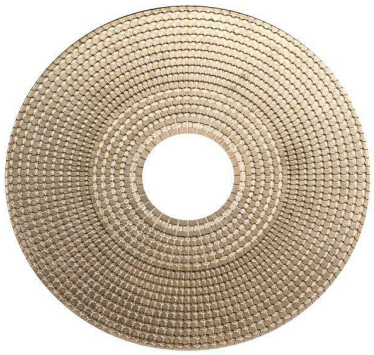

Fig.S3. 2D acoustic cloak based on acoustic circuit network

Layer	l_r(mm)	l_φ(mm)	V(mm^3)
1	2.05	0.10	3.00
2	1.54	0.13	2.43
3	1.37	0.22	2.29
4	1.37	0.31	2.18
5	1.24	0.41	2.06
6	1.24	0.25	2.06
7	1.24	0.30	2.06
8	1.24	0.36	2.06
9	1.24	0.41	2.06
10	1.24	0.46	2.06
11	1.24	0.52	2.06
12	1.24	0.57	2.06
13	1.24	0.63	2.06
14	1.24	0.69	2.06
15	1.24	0.74	2.06
16	1.24	N/A	N/A

Table1. Geometry parameters of the sample

Experimental Setup

To demonstrate the shielding phenomena, the sample is placed in a water tank to measure the pressure fields in the immediate environment of the cloaked object to compare with those without cloak. The tank edge is filled with absorbing rubber to reduce reflection. Because of the high impedance contrast between water and air as well as between water and glass, the system provides a 2D waveguide to confine the ultrasound wave propagation. Fig. S4 presents the pressure field distribution at 60 kHz without any object in the water tank. The side of the cloak machined with the network structure is placed against the bottom of the tank. The cloak has a thickness of 3mm with the depth of the cavities smaller than 1.36 mm. The water inside the cloak is connected to the surrounding water which is 1.5 mm deep through the channels along the radial direction around the outer boundary of the cloak.

The ultrasound signal from a spherical shape transducer is launched to the water as a point source. A waveform generator (Tektronix AFG 310) is used to drive the transducer. The source generated a burst of sine waves with a width of 20 periods. The pressure field around the cloak sample in the water is detected by a miniature hydrophone (RESON TC4038-1), amplified by Stanford research systems model SR650 and captured using a digital oscilloscope (Agilent DSO6104A) and then downloaded to a computer for post processing and analysis. The hydrophone is attached to a motorized translation stage. The control program of a customized LabVIEW scans across the data acquisition region by moving the hydrophones in a small increment 3mme to record the spatiotemporal distribution of the pressure field. The snapshot of the field pattern can be plotted as a function of position. To verify the broad operational bandwidth of the acoustic cloak, the transducer is excited over a discrete set of frequencies to illuminate the sample. The transducer operating spectrum limits us to test the frequency range from 52 kHz to 64 kHz.

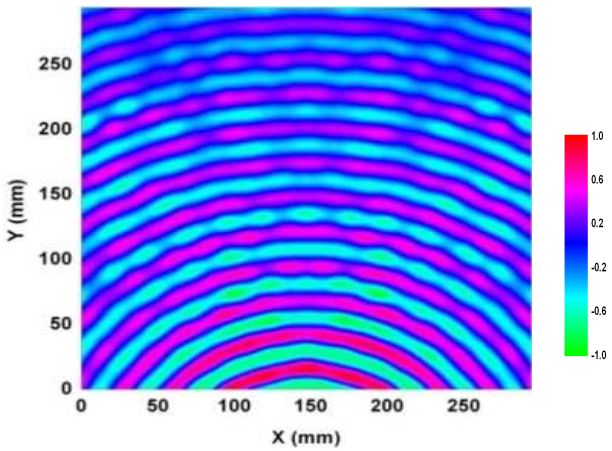

Fig.S4. Measured acoustic wave field distribution with a point source at 60 kHz in the water tank without any objects

Field Plots and Control Measurement

With the same measurement as in Fig.3, Fig.S5 presented the acoustic wave field maps at different frequency to demonstrate the cloaking functionality. The scattering shadow caused by the steel cylinder as shown in Fig.S5 (a-d) is reduces by the surrounding cloak in Fig.S5 (e-h) at frequency 54, 56, 58 and 62 kHz respectively. Due to the utilization of the non-resonant building blocks in the metamaterial cloak, the performance of cloak is not dependent on frequency. Theoretically, the cloak is expected to exhibit a broadband of operation from 40 to 80 kHz. However, we can only measure the cloaking behavior from 52 to 64 kHz in the experiment due to the limitation the experimental apparatus.

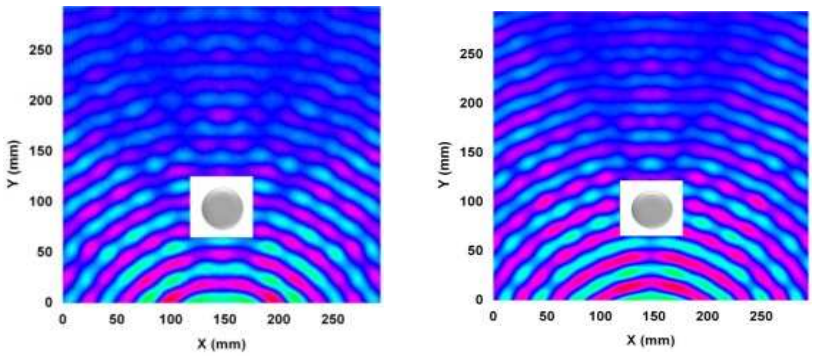

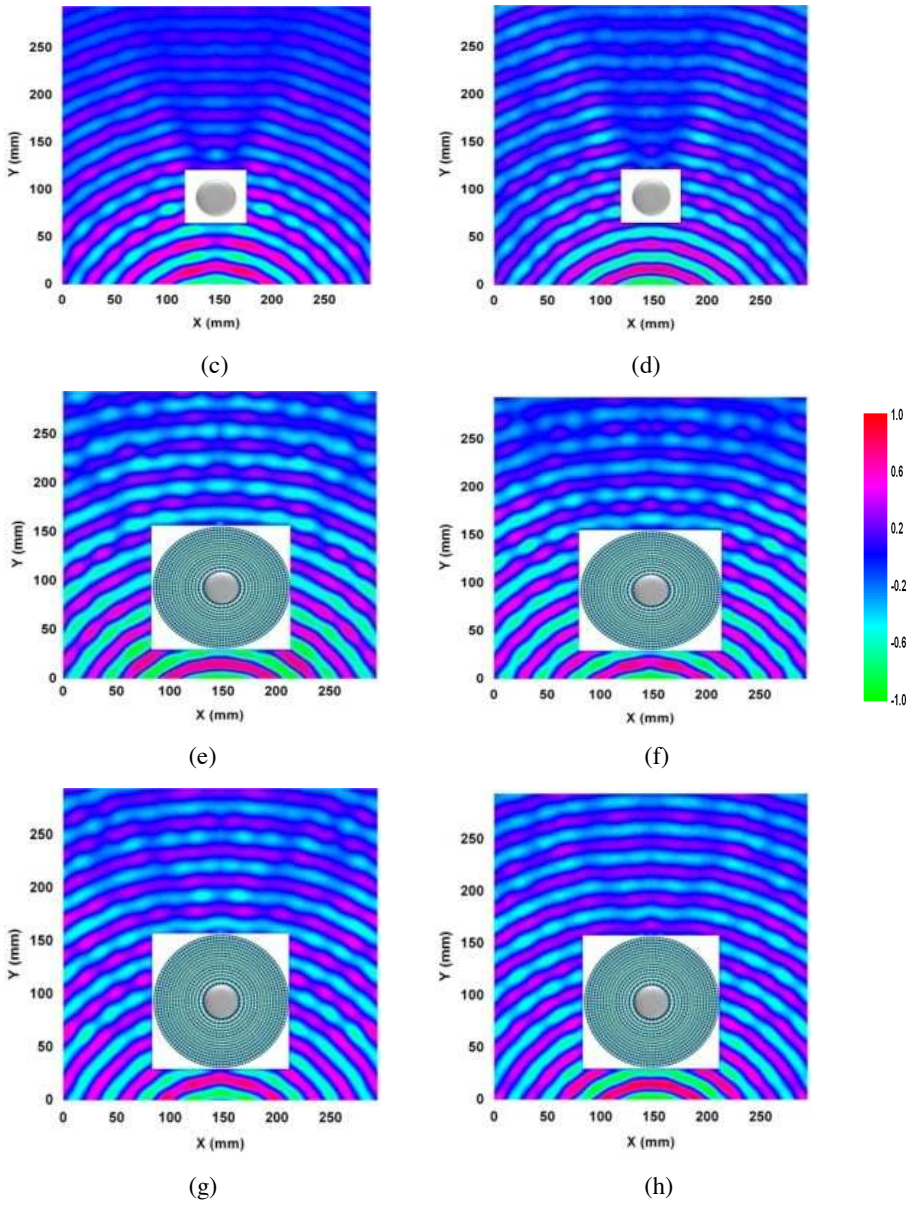

Fig.S5. Measured acoustic wave field mappings of two cases: with bare steel cylinder at (a) 54 kHz (b) 56 kHz (c) 58 kHz and (d) 62 kHz and when the steel cylinder is surrounded by the metamaterial cloak at (e) 54 kHz (f) 56 kHz (g) 58 kHz and (h) 62 kHz.

As a control experiment, we measured the field patter scattered by a steel cylinder with the same dimension as the cloak but with no network structure at 60 kHz. The result is shown in Fig. S6, strong scattering and large shadow area are observed behind the cylinder. The visibility of this cylinder is 1.38, which is much larger than 0.32 for the cloaked object whereas the hidden object in center has visibility of 0.56. This demonstrates that the steel cylinder without the designed structure actually causes more significant scattering

than the smaller cylinder which is hidden inside the cloak. Only with the machined building blocks, the cylindrical cloak can guide the acoustic wave to reform the wavefronts on the exit side.

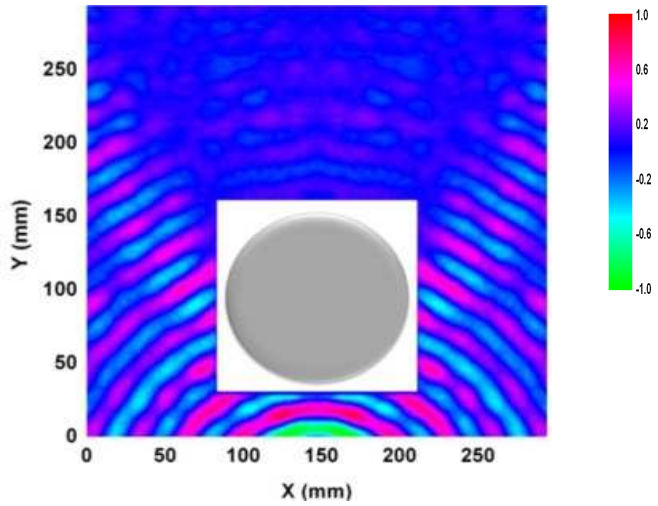

Fig. S6. Measured acoustic wave field distribution in the vicinity of a steel cylinder with the same geometry as the cloak

Numerical Simulation

To further demonstrate the effectiveness of our acoustic anisotropic metamaterial based on lumped circuit network, we simulated the acoustic wave propagation through the acoustic circuit network to compare with the results using finite element method (FEM) software COMSOL. In the FEM model, the cloak is approximated by 16 layers of homogeneous cylinders with the reduced cloaking parameters. In the circuit model, the cloak, hidden cylinder and the background water are all discretized and simulated by the circuit network. The number of unit cells for the cloak is set as same as the sample in the experiment. Comparison of Fig. S7 (a) and (b) indicates a good match between those two numerical approaches. More distortion is observed in the circuit model in Fig. S7 (b). This is mainly due to the difference in the boundary conditions. In COMSOL model, perfect matched layer is utilized to have zero reflection from the boundary, while in the circuit model the matching resistors are used to terminate the cells in the boundary.

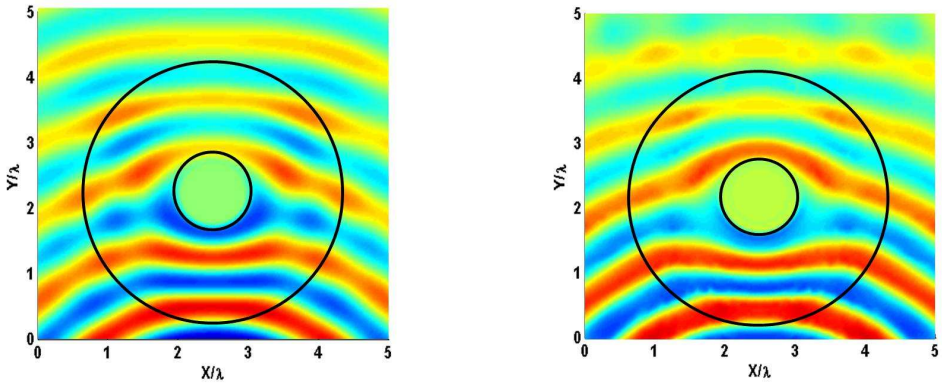

(a) (b)

Fig.S7. 2D simulations for the acoustic cloak with reduced material parameters with black lines indicating the inner and outer boundary of the cylindrical cloak. (a) The FEM simulation by software COMSOL. The cloak is approximated by 16-step piecewise homogeneous cylinders. (b) Lumped circuit model simulation of the cylindrical cloak performed by software SPICE.

REFERENCES

[1] A. Grbic, G. V. Eleftheriades', "Overcoming the diffraction limit with a planar left-handed transmission-line lens", *Phys. Rev. Lett.*, 92, 117403 (2004)

[2] Pendry J B, Schurig D and Smith D R ," Controlling Electromagnetic Fields ", *Science* **312** ,1780 (2006)

[3] S.Zhang et al, *Phys.Rev. Lett* **100,** 123002 (2008).

[4] G. W. Stewart, "Acoustic wave filters", *Phys.Rev.***20**, 528 (1922).

[5] W. P. Mason, "A study of the regular combination of acoustic elements, with applications to recurrent acoustic filters, tapered acoustic filters, and horns", Bell Syst. Tech. J . **6**, 258 (1927).

[6] L.L.Beranek, Acoustics, 1954, McGRAW-HILL,New York.

[7] L. E. Kinsler, Fundamentals of Acoustics, 1982, Wiley,New York.

[8] C.R. Fuller and F. J. fahy, "Characteristics of wave propagation and energy distributions in cylindrical elastic shells filled with fluid" *Journal of Sound and Vibration* **81**(4), 501-518, (1982)

[9] H. LAMB, "On the velocity of sound in a tube, as affected by the elasticity of the walls." *Manchester Literary and Philosophical Society-Memoirs and Proceedings*, **42**(9), (1898)

Layer	l_r(mm)	l_φ(mm)	$V(\mathrm{mm}^3)$
1	2.05	0.10	3.00
2	1.54	0.13	2.43
3	1.37	0.22	2.29
4	1.37	0.31	2.18
5	1.24	0.41	2.06
6	1.24	0.25	2.06
7	1.24	0.30	2.06
8	1.24	0.36	2.06
9	1.24	0.41	2.06
10	1.24	0.46	2.06
11	1.24	0.52	2.06
12	1.24	0.57	2.06
13	1.24	0.63	2.06
14	1.24	0.69	2.06
15	1.24	0.74	2.06
16	1.24	N/A	N/A